RESEARCH ARTICLE

The *Zic2* Gene Directs the Formation and Function of Node Cilia to Control Cardiac Situs

Kristen S. Barratt, Hannah C. Glanville-Jones, and Ruth M. Arkell*

Early Mammalian Development Laboratory, Research School of Biology, Evolution, Ecology and Genetics, The Australian National University, Canberra, ACT 0200, Australia

Received 18 December 2013; Revised 13 February 2014; Accepted 25 February 2014

Summary: The first molecular herald of organ asymmetry during murine embryogenesis is found at the periphery of the node in early-somite stage embryos. Asymmetric gene expression and calcium accumulation at the node occurs in response to a left-ward flow of extracellular fluid across the node, generated by motile cilia within the pit of the node and likely sensed by immotile cilia in the periphery of the node. The ciliation of node cells is controlled by a cascade of node-restricted transcription factor activity during mid-late gastrulation. Mutation of the murine Zic2 transcription factor is associated with random cardiac situs and a loss of asymmetric gene expression at the early-somite node and in the lateral plate. *Zic2* is not expressed in these regions but is transiently expressed in the mid-late gastrula node at the time of ciliogenesis. The cilia of the node are overtly abnormal in *Zic2* mutant embryos being dysmorphic and short relative to wild-type littermates. The expression of the *Noto*, *Rfx3*, and *Foxj1* transcription factors known to regulate ciliogenesis is greatly depleted in the mid-gastrula node of mutants, as is the expression of the *Pkd1l1* gene required for cilia function. Zic2 appears to be a component of the gene regulatory network that drives ciliation of node cells during gastrulation. genesis 52:626–635, 2014. © 2014 Wiley Periodicals, Inc.

Key words: mouse; gastrulation; heart; heterotaxy; laterality disorder; node; holoprosencephaly

INTRODUCTION

The *Zic2* gene is one of a family of five *Zic* genes in mammals each of which encodes a zinc finger containing, multifunctional transcription regulator (Ali *et al*., 2012; Houtmeyers *et al*., 2013). Germ-line mutation of this gene (*Zic2* in mouse and *ZIC2* in humans) causes a severe defect in forebrain development known as holoprosencephaly (HPE) in both man and mouse (Brown *et al*., 2005; Warr *et al*., 2008) with loss-of-function (LOF) the most likely cause of pathogenesis (Roessler *et al*., 2009). HPE arises when the Shh signal (normally emitted from the midline tissue known as the prechordal plate) is not received by the overlying neurectoderm. This failure could occur because the prechordal plate is not formed, because the Shh signal is defective or because the neurectoderm cannot receive or interpret the Shh signal. Previous analysis of mouse embryos homozygous for a severe LOF allele of *Zic2* (known as kumba; *Ku*) (Elms *et al*., 2003; Nolan *et al*., 2000) traced the aetiology of *Zic2*-associated HPE to a defect in the mid-gastrula node at 7.0 days postcoitum (dpc). This prevents the formation of the anterior notochord and ultimately results in a failure of prechordal plate development (Warr *et al*., 2008).

The murine node forms at the anterior of the primitive streak at mid-gastrulation. The cells that pass through the anterior primitive streak of the early-gastrula or the node give rise to the axial mesoderm of the embryonic midline (the axial mesoderm that underlies the forebrain is the prechordal plate, that which underlies the rest of the brain is the anterior notochord and that which underlies the spinal cord is the notochord). Cells that pass through the anterior primitive streak and later node also give rise to the majority of the definitive (or gut) endoderm. These anterior

* Correspondence to: Ruth Arkell, Research School of Biology, Building 46, The Australian National University, Canberra, ACT 0200, Australia. E-mail: ruth.arkell@anu.edu.au
Published online 2 March 2014 in Wiley Online Library (wileyonlinelibrary.com).
DOI: 10.1002/dvg.22767

primitive streak and node derived tissues, as well as cross-talk between them, are central to the formation of the head [for review see (Arkell and Tam, 2012)]. Embryos homozygous for the *Ku* allele of *Zic2* (*Zic2*$^{Ku/Ku}$) have apparently normal anterior primitive streak function with molecular abnormalities first detected at the stage of overt node formation (7.0 dpc). The expression of any gene so far examined that would normally be present in the 7.0 dpc node or its derivatives is greatly diminished in *Zic2*$^{Ku/Ku}$ embryos. Tissues derived from the later stage node (such as the trunk notochord) are more mildly affected in 9.5 dpc embryos (see Fig. 3O–R of Warr *et al*., 2008) suggesting that the defect in node gene expression and function is transient.

In addition to its role in anterior–posterior (A–P) and dorsal–ventral (D–V) patterning, the node and its derivatives are also intimately involved in the establishment of the left-right (L-R) axis (Hirokawa *et al*., 2012; Lee and Anderson, 2008; Norris, 2012). In the 24 h following the initial appearance of the node it develops into a shallow, crescent-shaped depression on the ventral side of the embryo. The cells within the depression are referred to as pit cells, whereas those that form the raised surface that rings the pit are called crown cells (Bellomo *et al*., 1996). Each pit and crown cell in the ventral layer of the node carries a monocilium on its apical surface that extends into the extracellular space (Lee and Anderson, 2008; Sulik *et al*., 1994). The cilia of the pit cells rotate in a clockwise direction and support a flow of extracellular fluid toward the left side of the node (called nodal flow) that is posited to establish differential signal(s) on the left and right of the node (Nonaka *et al*., 1998, 2002). The cilia on the crown cells are generally immotile, and these sensory cilia are thought to interpret the signal(s) established via nodal flow (McGrath *et al*., 2003). By the end of this 24 h period (i.e., at 8.0 dpc), the first known molecular asymmetries are detected within the crown cells of the node: expression of the secreted signaling molecule *Nodal* becomes elevated in crown cells on the left side whereas expression of *Dand5* (formerly *Cerl2*) a secreted Nodal antagonist becomes decreased at the left crown cells (Collignon *et al*., 1996; Lowe *et al*., 1996; Marques *et al*., 2004; Pearce *et al*., 1999). At the same time, intracellular Ca^{2+} becomes elevated at the left boundary of the node (McGrath *et al*., 2003). Subsequently, asymmetric signals are propagated to the left lateral plate mesoderm (LPM), via an unresolved mechanism. By the three-somite stage of development (8.25 dpc), Nodal signaling in the left LPM has induced its own expression, as well as that of the *Lefty2* Nodal antagonist and of the *Pitx2* transcription factor in an event known as the Nodal cascade (Shiratori and Hamada, 2006). The expression of another Nodal antagonist, *Lefty1*, at the embryonic midline forms a barrier that prevents the spread of the Nodal cascade to the right LPM (Meno *et al*., 1998).

Given that *Zic2* is required to execute the A–P and D–V components of node function, it may be anticipated that the node and midline formation defects in *Zic2*$^{Ku/Ku}$ embryos would interfere with L-R axis formation. This is supported by the observations that some homozygous embryos have incorrect heart morphology at 9.5 dpc (see Fig. 3O and P of Warr *et al*., 2008) and that approximately 5% of human *ZIC2*-associated HPE probands have cardiac abnormalities (Solomon *et al*., 2010). Here, we report that approximately half of *Zic2*$^{Ku/Ku}$ embryos have cardiac situs defects; a finding consistent with randomisation of L-R axis formation. Examination of *Zic2*$^{Ku/Ku}$ embryos at 8.5 dpc revealed the asymmetric expression of *Nodal*, *Lefty2*, and *Pitx2* in the left LPM is lost or greatly diminished, as is the expression of *Lefty1* at the midline, indicative of a failure of the Nodal cascade. Additionally, at 8.0 dpc, molecular readouts of nodal flow (*Nodal* and *Dand5* crown cell expression) are aberrant in 8.0 dpc *Zic2*$^{Ku/Ku}$ embryos, suggesting that the events required to generate left-biased signal(s) at the embryonic midline are compromised by the loss of *Zic2* function. In support of this hypothesis, node abnormalities are seen in mutant embryos. Nodal cilia form in *Zic2*$^{Ku/Ku}$ embryos but are shorter than in the equivalent staged wild-type and/or *Zic2*$^{Ku/+}$ littermates and the expression of genes known to be required for cilia formation and function (*Noto*, *Rfx3*, *Foxj1*, and *Pkd1L1*) is greatly down regulated in the node of *Zic2*$^{Ku/Ku}$ embryos. Evidently, the mid-gastrula node dysgenesis in *Zic2*$^{Ku/Ku}$ embryos also affects genes required for cilia formation and function and this may impair both nodal flow and signal perception. *Zic2*, therefore, acts early in node development to direct the expression of genes required for the establishment of all three embryonic axes.

RESULTS

Cardiac Situs is Randomized in *Zic2*$^{Ku/Ku}$ Embryos

To determine whether the previously characterized defect in midline development in *Zic2*$^{Ku/Ku}$ embryos impacts formation of the L-R embryonic axis, the direction of heart looping was scored in 9.5 dpc embryos ($N = 14$ *Zic2*$^{+/+}$, $N = 41$ *Zic2*$^{Ku/+}$, and $N = 16$ *Zic2*$^{Ku/Ku}$) following whole mount in situ hybridization (WMISH) to *Nppa*. This gene is expressed in the right atrium and left ventricle (Moorman and Christoffels, 2003) and was used to confirm the identity of heart regions. All wild-type, heterozygous and 56% of *Zic2*$^{Ku/Ku}$ embryos presented with dextral looping (Fig. 1a,d), whereas 31% of *Zic2*$^{Ku/Ku}$ embryos exhibited a leftward curve of the heart tube (sinistral looping, Fig. 1b,e) and the remaining 13% of *Zic2*$^{Ku/Ku}$ embryos had

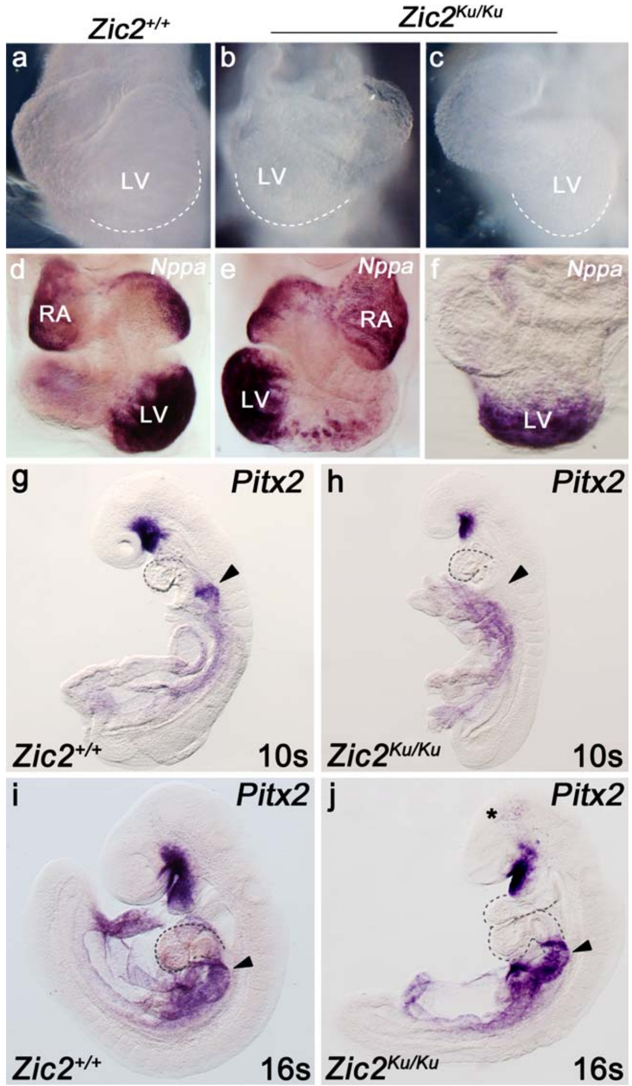

FIG. 1. *Zic2$^{Ku/Ku}$* embryos exhibit cardiac situs defects. **(a–c)** Dark-field images of hearts from embryos with 21 somites in ventral view; the dotted line shows the extent of the heart tube. **(a)** Wild-type heart formation (dextral looping). **(b)** A *Zic2$^{Ku/Ku}$* embryo with reverse heart formation (sinistral looping). **(c)** A *Zic2$^{Ku/Ku}$* embryo with abnormal forward looping (ventral looping). **(d–f)** Images of hearts following WMISH to *Nppa* to confirm chamber identity. **(d)** A 25 somite *Zic2$^{+/+}$* embryo with dextral looping. **(e)** A 25 somite *Zic2$^{Ku/Ku}$* embryo with sinistral looping**. (f)** A 16 somite *Zic2$^{Ku/Ku}$* embryo with ventral looping. **(g–j)** Lateral view of embryos following WMISH to *Pitx2*. **(g)** A 10 somite *Zic2$^{+/+}$* embryo with *Pitx2* transcription in the left cardinal vein (arrowhead). **(h)** A 10 somite *Zic2$^{Ku/Ku}$* embryo lacking *Pitx2* cardinal vein expression (arrowhead). **(i)** A 16 somite *Zic2$^{+/+}$* embryo with *Pitx2* transcription in the left cardinal vein (arrowhead). **(j)** A 16 somite *Zic2$^{Ku/Ku}$* embryo with sinistral heart looping, *Pitx2* transcription in the left cardinal vein (arrowhead) and ectopic forebrain expression (asterisk). LV: left ventricle, RA: right atrium. Dotted line indicates heart looping.

a heart tube that looped forward (ventral looping, Fig. 1c,f).

The mid-gestation demise of *Zic2$^{Ku/Ku}$* embryos (Elms *et al*., 2003) prevented the direct scoring of later asymmetric organs. Stereotypic cardinal vein morphology, however, occurs in response to left-right axis establishment and can be independent of heart looping. For example, defects in cardinal vein morphology occur in conjunction with other organ asymmetries such as lung isomerisms and mislocation of the pancreas in embryos that lack *Pitx2* (Shiratori *et al*., 2006). *Pitx2* is expressed in the left cardinal vein (Meno *et al*., 1998) and was used as a surrogate marker for the correct establishment of asymmetries other than heart looping. At 9–9.5 dpc, *Pitx2* is expressed in the cardinal vein on the left, but not right, of wild-type embryos (Fig. 1g,i). Left cardinal vein expression of *Pitx2* was detected in the majority of *Zic2$^{Ku/Ku}$* embryos, but some embryos lacked this expression domain, independent of the direction of heart looping (Fig. 1h,j). This suggests that aspects of L-R organ development other than heart looping may be affected in *Zic2$^{Ku/Ku}$* embryos. Interestingly, ectopic expression of *Pitx2* could be seen in the midbrain of 9.5 dpc *Zic2$^{Ku/Ku}$* embryos (Fig. 1j). *Pitx2* is expressed in the ventral diencephalon (Martin *et al*., 2002), but not until 10.5 dpc, and wild-type stage-matched embryos did not have corresponding *Pitx2* expression.

The Nodal Cascade is Absent in *Zic2* Mutant Embryos

Overt L-R axis formation is preceded by the asymmetric expression of certain genes in the LPM and by the establishment of a midline barrier. At the 3–6 somite stage of development the secreted molecule *Nodal*, its secreted antagonist *Lefty2* and the downstream transcription factor *Pitx2* are all expressed in the left LPM and the *Lefty1* Nodal antagonist is expressed at the midline. Examination of the expression of these genes in early somite stage embryos via WMISH demonstrated that each consequence of Nodal signaling is severely compromised in *Zic2$^{Ku/Ku}$* embryos. The expression of *Nodal* was detected at the node but not in the LPM of 3-somite mutant embryos (Fig. 2a,b) and likewise *Lefty2* (Fig. 2c,d) expression was not detected in the LPM. The expression of *Pitx2* was detected throughout the entire A–P extent of the LPM in wild-type embryos with 3–5 somites, whereas it was only weakly detected in the anterior LPM of equivalent stage *Zic2$^{Ku/Ku}$* embryos (Fig. 2e,f). The apparent ability to initiate anterior LPM *Pitx2* expression in the absence of *Nodal* expression suggests loss of *Zic2* function reveals a Nodal independent mechanism of *Pitx2* expression initiation. The expression of *Lefty1* at the embryonic midline was severely depleted in early somite-stage *Zic2$^{Ku/Ku}$* embryos (Fig. 2c,d). The absence of the midline barrier in the presence of the asymmetric signal is typically associated with the bilateral establishment of the Nodal cascade (i.e., bilateral expression of *Nodal*, *Lefty2*, and

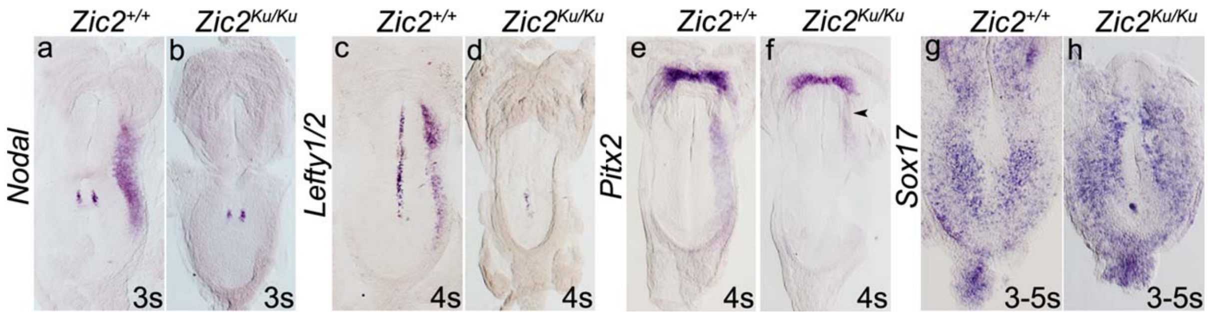

FIG. 2. The Nodal cascade and midline barrier are compromised in *Zic2*$^{Ku/Ku}$ embryos. Ventral views of embryos following WMISH to the genes shown on embryos of the genotypes and stage shown. Anterior is to the top in all images, only the caudal half of the embryo is shown in (**g**) and (**h**). **(a and b)** *Nodal* is normally expressed in the crown cells of the node and in the left LPM; the LPM expression is absent in *Zic2*$^{Ku/Ku}$ embryos**. (c, d)** *Lefty1* is normally expressed in the midline rostral of the node and *Lefty2* in the left LPM; *Lefty1* expression is depleted and *Lefty2* expression lost in *Zic2*$^{Ku/Ku}$ embryos. **(e and f)** *Pitx2* is normally expressed bilaterally in the cranial mesenchyme and in the left LPM; the cranial mesenchyme expression is retained and residual expression is seen in the anterior left LPM of *Zic2*$^{Ku/Ku}$ embryos [arrowhead in (**f**)]. **(g and h)** *Sox17* is normally expressed in the definitive endoderm; this expression is retained in *Zic2*$^{Ku/Ku}$ embryos. S: somites.

Pitx2) (Meno *et al*., 1998; Yamamoto *et al*., 2003). The near absence of both the midline barrier and LPM expression of *Nodal*, *Lefty2*, and *Pitx2* suggests that the asymmetric signal is generated and perceived but not transferred to the LPM or that it is not correctly established.

Definitive Endoderm Formation in *Zic2* Mutant Embryos

The correct formation of the definitive endoderm is required to transfer the asymmetric signal(s) to the LPM and embryos lacking *Sox17* are unable to complete this process (Viotti *et al*., 2012). The definitive endoderm of *Zic2*$^{Ku/Ku}$ embryos is aberrant at mid-late gastrulation (Warr *et al*., 2008) and may be incompetent for signal transfer. WMISH to *Sox17* revealed no difference in expression between wild-type and mutant embryos (Fig. 2g,h), suggesting the definitive endoderm is capable of signal transmission.

Node Function and Cilia Development is Compromised in *Zic2* Mutant Embryos

To determine whether the asymmetric midline signal is effectively established, gene expression at the node of early somite embryos was examined in stage-matched wild-type and mutant embryos. The expression of *Nodal* itself becomes asymmetric at the node of wild-type embryos slightly before the initiation of *Nodal* LPM expression (i.e., at the 0–2 somite stage). The perinodal expression domain of *Nodal* varied between homozygous *Ku* embryos, but was always different to that of stage-matched wild-type littermates (Fig. 3a–d). In all cases *Nodal* expression was diminished and in some cases expression failed to become asymmetric. Expression of another secreted molecule, the Nodal antagonist *Dand5*, also becomes asymmetric at the node of wild-type embryos prior to the initiation of *Nodal* LPM expression. The expression of *Dand5* was greatly depleted in the node of all *Zic2*$^{Ku/Ku}$ embryos examined and no asymmetric expression was observed (Fig. 3e–h). These data indicate that *Zic2* is genetically upstream of asymmetric gene expression at the node.

To determine whether the effects on gene expression at the node result from aberrant node development, we examined the node of 3–5 somite-stage embryos by light microscopy [differential interference contrast (DIC) optics] and the node of 0–3 somite-stage embryos by scanning electron microscopy (SEM). Visual inspection of the overall morphology of the node (shape and size) suggested that *Zic2*$^{Ku/Ku}$ nodes were smaller, however, measurement of the node circumference and length of the anterior–posterior axis were not found to be significantly different from wild-type nodes ($P > 0.05$, Fig. 3i–l). The cilia of node pit cells occurred at the same frequency (i.e., ~1 cilium/cell) across all genotypes ($P > 0.05$). Cilia length was overtly different (Fig. 3n,o) and when measured wild-type embryos were found to contain cilia with a mean length of 4 μm whereas *Zic2*$^{Ku/+}$ embryos had cilia with a mean length of 3.1 μm and *Zic2*$^{Ku/Ku}$ embryos had cilia with a mean length of 2.5 μm ($P < 0.01$). In addition, the cilia of *Zic2*$^{Ku/Ku}$ embryos were dysmorphic and often bulbous at the base (Fig. 3m–o). In combination with the gene expression data, this suggests that the node cilia do not retain sufficient function for symmetry breaking.

Zic2 Controls the Node Expression of Genes Required for Cilia Formation and Function

Zic2 is not expressed in the node of early somite stage embryos, whereas it is expressed in the node of mid-late gastrula embryos (Elms *et al*., 2004). As *Zic2* is a transcriptional regulator and expected to act cell-autonomously, we hypothesized that *Zic2* is required to

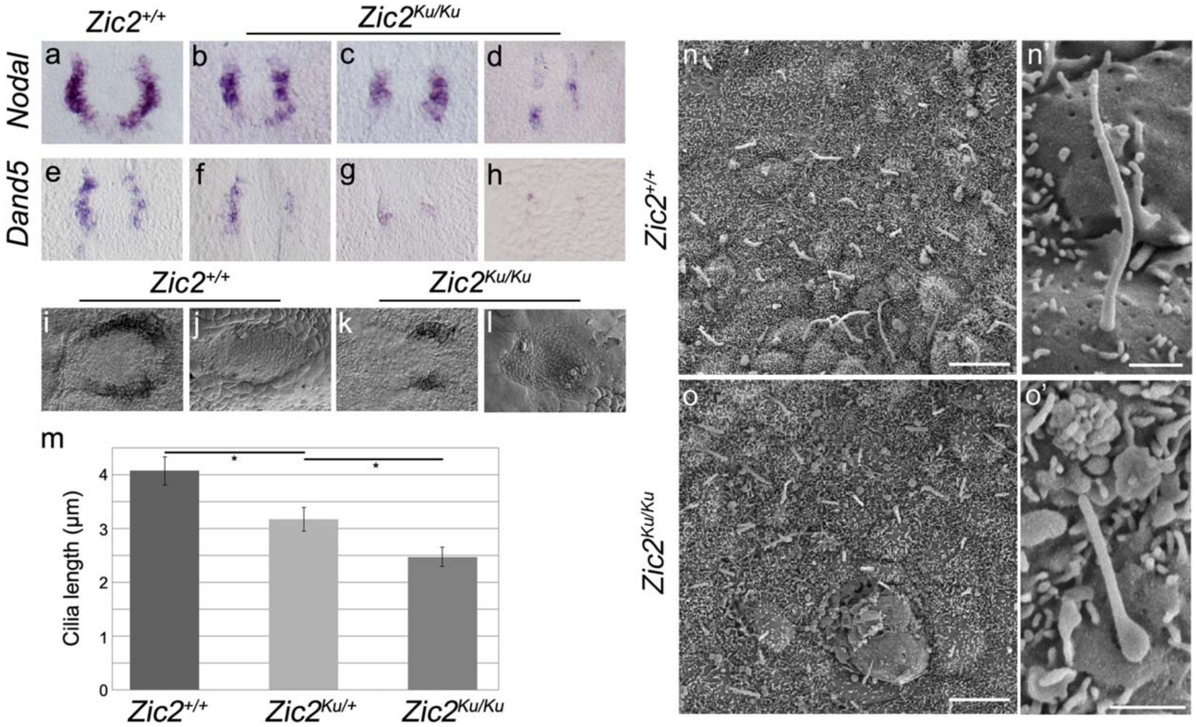

FIG. 3. Aberrant gene expression and cilia morphology in the early somite node of *Zic2*$^{Ku/Ku}$ embryos. Ventral view of 3–5 somite embryos of the genotypes shown following WMISH to the genes shown. Anterior is to the top. **(a–d)** *Nodal* expression normally becomes asymmetric in wild-type two somite embryos; the perinodal expression is diminished and/or fails to become asymmetric in *Zic2*$^{Ku/Ku}$ embryos. **(e–h)** *Dand5* is asymmetrically expressed in the crown cells of the node in wild-type two somite embryos; the perinodal expression is diminished and fails to become asymmetric in *Zic2*$^{Ku/Ku}$ embryos. **(l and k)** DIC, and **(j and l)** SEM images of node morphology in embryos of the genotypes shown; ventral view, anterior is to the left. The length of *Zic2*$^{Ku/Ku}$ nodes is not distinguishable from wild-type. **(m)** A column graph depicting the mean cilia length in 0–3 somite embryos of different genotypes. Error bars: SEM, *: $P < 0.01$, Fisher's LSD ANOVA **(n–o′)** SEM images of node cilia in 3–4 somite embryos of the genotypes shown. Scale bar: 5 μm (n, o) and 1 μm (n′, o′).

(either directly or indirectly) regulate the expression of genes required for node and cilia formation and function in the gastrula. We have previously shown that the expression of *Foxa2* in the mid-gastrula node is severely depleted (Warr *et al*., 2008) and it is known that embryos lacking *Foxa2* are unable to form a functional node (Ang and Rossant, 1994). To determine whether this early defect in Node function may also influence L-R axis formation, we examined the expression of genes required for node ciliogenesis (*Noto*, *Rfx3*, and *Foxj1*) (Beckers *et al*., 2007; Bonnafe *et al*., 2004; Zhang *et al*., 2004) and sensory function (*Pkd1l1*) (Field *et al*., 2011). As shown in Fig. 4, the expression of each of these genes is severely depleted in 7.0 and 7.5 dpc embryos, suggesting (as before; Warr *et al*., 2008) widespread dysgenesis of the node of mid-gastrula *Zic2*$^{Ku/Ku}$ embryos.

DISCUSSION

We have previously shown that *Zic2* dependent transcription is required for correct function of the 7.0 dpc node (Brown *et al*., 2005; Warr *et al*., 2008). Consistent with this, *Zic2* is transiently expressed in the node. Transcripts are first detected at 7.0 dpc, before allantoic bud development, just as the cells of the anterior primitive streak reach the distal egg cylinder and the patent node forms. Transcripts persist for the next 12–16 h, being undetectable by the time the node has formed a pit in the outer curvature of the 7.75 dpc embryo (Elms et al. 2004). The cells that pass through the node during this time form one region of the axial mesoderm (the anterior notochord) and the majority of the definitive endoderm. The development of the anterior notochord is compromised in *Zic2*$^{Ku/Ku}$ embryos. This apparently halts prechordal plate development and leads to HPE (Warr *et al*., 2008). Here, we show that this early defect in node development also compromises the establishment of the L-R embryonic axis. The *Zic2* transcription factor evidently acts upstream of the expression of genes known to regulate ciliogenesis and function, as the expression of these genes within the node is greatly depleted. The pit cells within the node of embryos that lack *Zic2* function have short, dysmorphic cilia relative to their wild-type, stage-matched littermates and the molecular hallmarks of symmetry breaking at the embryonic midline are abnormal. Subsequently, the nodal signaling cascade within the left LPM fails and cardiac situs is randomized.

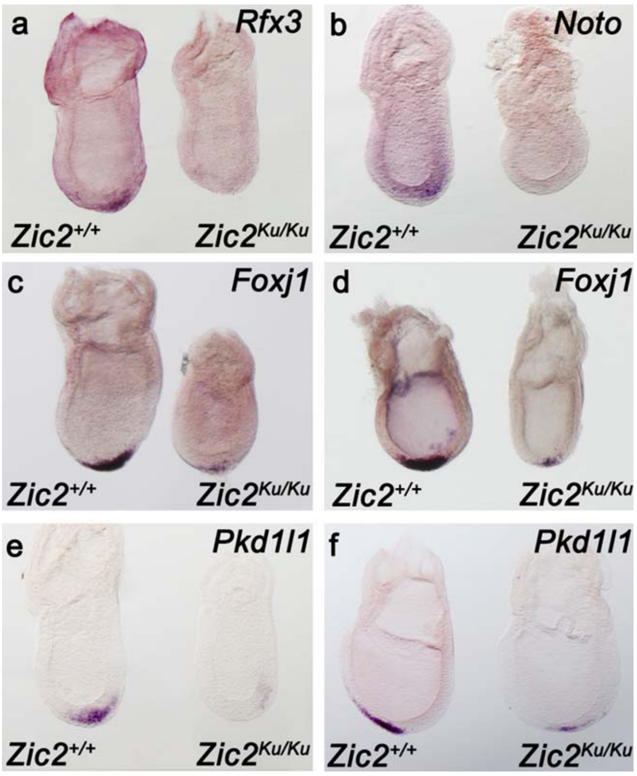

FIG. 4. Aberrant gene expression in the mid-gastrula node of *Zic2*$^{Ku/Ku}$ embryos. Lateral views of embryos following WMISH to the genes shown on embryos of the genotypes shown. Anterior is to the left. **(a)** 7.0 dpc, preallantoic bud stage embryos, *Rfx3* node expression is diminished in *Zic2*$^{Ku/Ku}$ embryos. **(b)** 7.0 dpc, preallantoic bud stage embryos, *Noto* node expression is diminished in *Zic2*$^{Ku/Ku}$ embryos. **(c)** 7.0 dpc, preallantoic bud stage embryos, and **(d)** 7.5 dpc, early allantoic bud stage embryos; *Foxj1* node expression is diminished in the *Zic2*$^{Ku/Ku}$ embryos. **(e)** 7.0 dpc, preallantoic bud stage embryos, and **(f)** 7.75, late allantoic bud stage embryos; *Pkd1l1* node expression is diminished in the *Zic2*$^{Ku/Ku}$ embryos.

Node cells first become visible on the outside of the embryo at 7.0 dpc and contain a centrally located, short cilium as they emerge from beneath the outer endoderm (Lee and Anderson, 2008). Three transcription factors that are expressed at the forming node and are required for the production of functional node cilia in mice have already been identified via mutagenesis studies. Mutation of either the *Foxj1* or *Rfx3* transcription factors is associated with defective L-R axis development (Bonnafe *et al.*, 2004; Zhang *et al.*, 2004). A combination of mutagenesis and transcriptional profiling experiments in a variety of model organisms has led to the conclusion that *Foxj1* expression is necessary for the biogenesis of motile cilia, whereas Rfx proteins are necessary to assemble both motile and immotile cilia (Thomas *et al.*, 2010). The node expression of both *Foxj1* and *Rfx3* is greatly depleted in 8.0 dpc mouse embryos that lack the homeobox containing *Noto* transcription factor and *Noto*$^{-/-}$ embryos have short, malformed, and immotile cilia (Beckers *et al.*, 2007). Moreover, the cilia phenotype of *Noto* null embryos can be rescued by *Foxj1* insertion into the *Noto* locus (Alten *et al.*, 2012), suggesting that *Noto* may be upstream of *Foxj1* and *Rfx3*. Mutation of *Noto* does not affect A–P or D–V patterning and its function seems specific to the L-R axis component of node activity. In contrast, the *Zic2* transcription factor is required to pattern all three embryonic axes. In combination with the compromised expression of *Noto*, *Rfx3*, and *Foxj1* in *Zic2*$^{Ku/Ku}$ embryos, this suggests that *Zic2* may act upstream of all of these transcription factors to initiate node ciliogenesis.

Embryos that lack *Noto*, *Foxj1*, or *Rfx3* have disrupted L-R axes formation and presumably have compromised nodal flow due to cilia malformation, but they are often able to initiate the Nodal cascade within the LPM (with cases of left, right, or bilateral expression found in combination with a proportion of embryos that fail to show LPM expression of the relevant marker genes) (Beckers *et al.*, 2007; Bonnafe *et al.*, 2004; Zhang *et al.*, 2004). A follow-up study of *Rfx3* mutants indicated that the phenotype variability may correlate with the degree of cilia malformation and of nodal flow and it has been proposed that even a weak nodal flow is sufficient to generate asymmetric gene expression at the node (Shinohara *et al.*, 2012). None-the-less, the variable ability to initiate the Nodal cascade is in contrast to the *Zic2*$^{Ku/Ku}$ embryos in which indicators of the Nodal cascade in both the LPM and midline were almost entirely absent and neither right-sided nor bilateral expression of *Nodal*, *Lefty2*, or *Pitx2* was ever observed in embryos with 3–5 somites. There are at least two possible factors that may account for this more severe phenotype of the *Zic2* mutant. One is that all *Zic2*$^{Ku/Ku}$ embryos have no nodal flow (whereas some *Noto*, *Foxj1*, and *Rfx3* mutants generate at least a small amount of nodal flow). This could occur because of a difference in the target gene sets of these transcription factors, or because of genetic background effects. Experiments that examine the precise structure of the dysmorphic cilia or that examine cilia motility or measure nodal flow in the *Zic2*$^{Ku/Ku}$ mutants have not been conducted. Although the cilia of embryos lacking *Noto* or *Foxj1* have been shown to be short, with structural defects and be mainly immotile (Alten *et al.*, 2012; Beckers *et al.*, 2007), nodal flow has not been measured in these mutants. To fully explore the hypothesis, that nodal flow is more severely compromised in the *Zic2* mutants than in *Noto*, *Foxj1*, or *Rfx3* mutants all alleles would need to be bred onto the same genetic background and cilia morphology, motility, and nodal flow systematically compared.

A second possible reason for the difference between the phenotype of the *Zic2* mutants and that of embryos lacking *Noto*, *Foxj1*, or *Rfx3* is raised by similarities between the phenotype of *Zic2*$^{Ku/Ku}$ embryos and that of embryos with LOF mutations of either *Pkd1l1* or *Pkd2* (Ermakov *et al*., 2009; Field *et al*., 2011; Pennekamp *et al*., 2002). LOF mutations in either of these genes result in a failure of the Nodal cascade, rather than in bilateral or random activation of the cascade. These related proteins (Pkd1L1 and Pkd2) physically interact and are colocated on cilia and are proposed to sense the left-biased signal at the node (Field *et al*., 2011; Yoshiba *et al*., 2012). The finding that *Pkd1l1* expression is depleted at the node of *Zic2*$^{Ku/Ku}$ embryos, suggests that the cilia of the *Ku* node may be compromised in their ability to respond to whatever nodal flow is generated in these embryos. It is possible that the failure of stereotypic cardiac situs in *Zic2*$^{Ku/Ku}$ embryos is caused by the cumulative effect of decreased nodal flow and decreased perception of flow.

The work presented here, indicates that a severe LOF *Zic2* allele is associated with cardiac abnormalities. Like the *Zic2*-associated HPE phenotype, cardiac abnormalities are found only in embryos homozygous for the *Ku* allele. Human patients with two mutated copies of *ZIC2* have never been identified and HPE can clearly be caused by LOF of one copy of *ZIC2* (Roessler *et al*., 2009). The reason for this apparent discrepancy between human and mouse genetics is not known, but it is commonly observed that mice are less sensitive to haploinsufficiency than humans (Bogani *et al*., 2005). It seems likely that at least a subset of human HPE patients with mutation of *ZIC2* will have cardiac and/or other defects of L-R axis formation and this is supported by the current clinical data (Solomon *et al*., 2010). Moreover, the observed incidence of *ZIC2*-associated cardiac defects would likely increase if this feature is specifically examined. Children presenting with *ZIC2*-associated HPE require examination for cardiac and other visceral situs problems. It is also possible that mutations in *ZIC2* will emerge as a risk factor for Heterotaxy once genome sequencing (rather than gene specific mutation detection) of proband DNA becomes the norm.

Zic2 is the second member of the Zic gene family to be associated with L-R axis formation; the *ZIC3* gene is mutated in X-linked Heterotaxy (Gebbia *et al*., 1997) and loss of *Zic3* function leads to L-R axis defects in mice, *Xenopus*, and zebrafish (Ahmed *et al*., 2013; Cast *et al*., 2012; Purandare *et al*., 2002). In the mouse, *Zic3* is expressed at the node of embryos from 8.0 dpc (headfold, presomite embryo) until at least the seven-somite stage (Elms *et al*., 2004). This expression first becomes apparent after *Zic2* node expression has ceased and the two genes are not coexpressed at the node. Mouse embryos null for *Zic3* initiate, but do not maintain *Nodal* expression at the node and expression of *Nodal* in the LPM is randomized with cases of left, right or bilateral expression (Purandare *et al*., 2002). The expression of a reporter transgene, driven by an upstream *Nodal* enhancer, is decreased in the *Zic3* null background, suggesting that *Nodal* may be a direct Zic3 target (Ware *et al*., 2006). However high resolution microscopy has revealed aberrant node and cilia morphology in *Zic3* mutant embryos (Sutherland *et al*., 2013) suggesting a primary role for Zic3 in or upstream of ciliogenesis and node development.

In conclusion, *Zic2* is required for L-R axis formation; most likely because it controls the expression of genes required for the formation and function of node cilia. Each of the other transcription factors known to be involved in this process (*Noto*, *Foxj1*, and *Rfx3*) uniquely affects the L-R axis formation component of node function. In contrast *Zic2* appears to act upstream of genes required for axial mesoderm as well as cilia formation and so influences the development of all three embryonic axes. It will be interesting to further position *Zic2* within the gene regulatory networks that direct axial mesoderm and node cilia formation.

METHODS

Mouse Husbandry, Strains, and Alleles

The kumba (*Ku*) allele of *Zic2* (Elms *et al*., 2003; Nolan *et al*., 2000) was maintained on two distinct backgrounds by continuous backcross to either C3H/HeH or 129/SvEv mice. In both cases, mice from backcross 10 or beyond were used for analysis. Gene expression and phenotype were found to be identical between the two backgrounds for both *Zic2*$^{Ku/+}$ and *Zic2*$^{Ku/Ku}$ embryos at embryonic stages 7.0–9.5 dpc and analysis of embryos was performed using mice derived from both colonies. Mice were maintained in a light cycle of 12 h light: 12 h dark, the midpoint of the dark cycle being 12 A.M. For the production of staged embryos, 12 P.M. on the day of the appearance of the vaginal plug is designated 0.5 dpc. Mice were genotyped by polymerase chain reaction (PCR) screening of genomic DNA extracted from ear biopsy tissue (Thomsen *et al*., 2012) and embryos were genotyped using a fragment of extra embryonic tissue/ectoplacental cone or yolk sac (depending on stage). Genomic DNA was extracted from embryonic tissue described previously (Arkell *et al*., 2001).<<?2>>

Whole Mount In Situ Hybridization

WMISH was performed as previously described (Elms *et al*., 2003) using mouse probes *Foxj1* [BC082543, (Cruz *et al*., 2010)], *Lefty1/2* (Meno *et al*., 1996), *Nodal* (Conlon *et al*., 1994), *Nppa* (IMAGE 402095, W77688), *Pitx2* (Ryan *et al*., 1998), *Pkd1l1* (Field *et al*., 2011), and *Sox17* (IMAGE 1529001, AW985818). The 888 bp mouse *Dand5* (previously *Cerl2*) fragment (NCBI ref. seq. NR_033145), the 472 bp mouse *Rfx3* fragment

(NCBI ref. seq. NM_011265) and the 368 bp *Noto* fragment (NCBI ref. seq. NM_001007472) were amplified from genomic DNA and individually cloned into pGEM T Easy (Promega). Template DNA was linearized and in vitro transcribed with the following: *SacII* and SP6 polymerase (*Dand5*), *NcoI* and SP6 polymerase (*Rfx3*), *SalI* and T7 polymerase *(Noto*). For each probe and stage of embryogenesis examined a minimum of four $Zic2^{Ku/Ku}$ embryos were compared to precisely stage-matched $Zic2^{+/+}$ littermates. Upon completion of the WMISH procedure, embryos were postfixed in 4% paraformaldehyde (PFA) and transferred via a glycerol series to 100% glycerol. For photography, embryos were flat-mounted under a glass coverslip and photographed in a Nikon SMZ 21500 Stereomicroscope and DS-Ri1 camera (Nikon).

DIC Microscopy

Fixed embryos were mounted under a glass coverslip in 100% glycerol and their node visualized with a 40× objective (Leica) in a compound microscope (Leica DM5500 FL DIC) using DIC optics. Images were captured using a Leica DFC365 FX camera and LAS V4.3 software.

Scanning Electron Microscopy

Mouse embryos at 8.0 dpc were dissected in 10% (v/v) fetal bovine serum in phosphate buffered saline (PBS) and fixed overnight in fresh 2% paraformaldehyde/2.5% gluteraldehyde/0.1 M cacodylate buffer (pH 7.4) at 4°C. After rinsing with 0.1 M cacodylate buffer, embryos were postfixed in 1% OsO_4/0.1 M cacodylate for 20 mins at room temperature. They were dehydrated through a graded EtOH series and dried at a critical point with a CPD010 (Balzers Union). Embryos were coated in platinum by an EMTECH K550X sputter coater. All imaging was performed on a Hitachi 4300SE/N FESEM at 3 kv.

Node Measurements and Statistical Analysis

Node morphology and size was examined using DIC optics on three embryos of each genotype ($Zic2^{+/+}$, $Zic2^{Ku/+}$, and $Zic2^{Ku/Ku}$). Node circumference and the length of the anterior–posterior axis were measured using LAS V4.3 software. Cilia frequency and length were counted in three embryos from each genotype ($Zic2^{+/+}$, $Zic2^{Ku/+}$, and $Zic2^{Ku/Ku}$) using SEM. For cilia frequency and length analysis, SEM images were recorded at 15,000× magnification. The file name of each image was altered to a number and the file order randomized by an independent worker so that the genotype of the embryo was unknown to the worker calculating cilia frequency and length. Cilia length was determined by measuring pixel length in Adobe Photoshop CS5 and conversion to μm (using a factor determined by the number of pixels per μm). In total, 10 node cilia were measured in each of three embryos per genotype. Fisher's LSD ANOVA was used to determine statistical significance of $P < 0.01$.

ACKNOWLEDGMENT

The authors thank Dominic Norris for providing several riboprobes and Carol Wicking and the ANU Centre for Advanced Microscopy for advice regarding scanning electron microscopy.

LITERATURE CITED

Ahmed JN, Ali RG, Warr N, Wilson HM, Bellchambers HM, Barratt KS, Thompson AJ, Arkell RM. 2013. A murine Zic3 transcript with a premature termination codon evades nonsense-mediated decay during axis formation. Dis Model Mech 6:755–767.

Ali RG, Bellchambers HM, Arkell RM. 2012. Zinc fingers of the cerebellum (Zic): Transcription factors and co-factors. Int J Biochem Cell Biol 44:2065–2068.

Alten L, Schuster-Gossler K, Beckers A, Groos S, Ulmer B, Hegermann J, Ochs M, Gossler A. 2012. Differential regulation of node formation, nodal ciliogenesis and cilia positioning by Noto and Foxj1. Development 139:1276–1284.

Ang SL, Rossant J. 1994. HNF-3 beta is essential for node and notochord formation in mouse development. Cell 78:561–574.

Arkell RM, Cadman M, Marsland T, Southwell A, Thaung C, Davies JR, Clay T, Beechey CV, Evans EP, Strivens MA, Brown SD, Denny P. 2001. Genetic, physical, and phenotypic characterization of the Del(13)Svea36H mouse. Mamm Genome 12:687–694.

Arkell RM, Tam PP. 2012. Initiating head development in mouse embryos: Integrating signalling and transcriptional activity. Open Biol 2:120030.

Beckers A, Alten L, Viebahn C, Andre P, Gossler A. 2007. The mouse homeobox gene Noto regulates node morphogenesis, notochordal ciliogenesis, and left-right patterning (vol 104, pg 15765, 2007). PNAS 104:17554–17554.

Bellomo D, Lander A, Harragan I, Brown NA. 1996. Cell proliferation in mammalian gastrulation: The ventral node and notochord are relatively quiescent. Dev Dyn 205:471–485.

Bogani D, Willoughby C, Davies J, Kaur K, Mirza G, Paudyal A, Haines H, McKeone R, Cadman M, Pieles G, Schneider JE, Bhattacharya S, Hardy A, Nolan PM, Tripodis N, Depew MJ, Chandrasekara R, Duncan G, Sharpe PT, Greenfield A, Denny P, Brown SD, Ragoussis J, Arkell RM. 2005. Dissecting the genetic complexity of human 6p deletion syndromes by using a region-specific, phenotype-driven mouse screen. PNAS 102:12477–12482.

Bonnafe E, Touka M, AitLounis A, Baas D, Barras E, Ucla C, Moreau A, Flamant F, Dubruille R, Couble P, Collignon J, Durand B, Reith W. 2004. The transcription factor RFX3 directs nodal cilium development and left-right asymmetry specification. Mol Cell Biol 24:4417–4427.

Brown L, Paraso M, Arkell R, Brown S. 2005. In vitro analysis of partial loss-of-function ZIC2 mutations in holoprosencephaly: Alanine tract expansion modulates DNA binding and transactivation. Hum Mol Gen 14:411–420.

Cast AE, Gao C, Amack JD, Ware SM. 2012. An essential and highly conserved role for Zic3 in left-right patterning, gastrulation and convergent extension morphogenesis. Dev Biol 364:22–31.

Collignon J, Varlet I, Robertson EJ. 1996. Relationship between asymmetric nodal expression and the direction of embryonic turning. Nature 381:155–158.

Conlon FL, Lyons KM, Takaesu N, Barth KS, Kispert A, Herrmann B, Robertson EJ. 1994. A primary requirement for nodal in the formation and maintenance of the primitive streak in the mouse. Development 120:1919–1928.

Cruz C, Ribes V, Kutejova E, Cayuso J, Lawson V, Norris D, Stevens J, Davey M, Blight K, Bangs F, Mynett A, Hirst E, Chung R, Balaskas N, Brody SL, Marti E, Briscoe J. 2010. Foxj1 regulates floor plate cilia architecture and modifies the response of cells to sonic hedgehog signalling. Development 137:4271–4282.

Elms P, Scurry A, Davies J, Willoughby C, Hacker T, Bogani D, Arkell R. 2004. Overlapping and distinct expression domains of Zic2 and Zic3 during mouse gastrulation. GEP 4:505–511.

Elms P, Siggers P, Napper D, Greenfield A, Arkell R. 2003. Zic2 is required for neural crest formation and hindbrain patterning during mouse development. Dev Biol 264:391–406.

Ermakov A, Stevens JL, Whitehill E, Robson JE, Pieles G, Brooker D, Goggolidou P, Powles-Glover N, Hacker T, Young SR, Dear N, Hirst E, Tymowska-Lalanne Z, Briscoe J, Bhattacharya S, Norris DP. 2009. Mouse mutagenesis identifies novel roles for left-right patterning genes in pulmonary, craniofacial, ocular, and limb development. Dev Dyn 238:581–594.

Field S, Riley KL, Grimes DT, Hilton H, Simon M, Powles-Glover N, Siggers P, Bogani D, Greenfield A, Norris DP. 2011. Pkd1l1 establishes left-right asymmetry and physically interacts with Pkd2. Development 138:1131–1142.

Gebbia M, Ferrero GB, Pilia G, Bassi MT, Aylsworth A, Penman-Splitt M, Bird LM, Bamforth JS, Burn J, Schlessinger D, Nelson DL, Casey B. 1997. X-linked situs abnormalities result from mutations in ZIC3. Nat Genet 17:305–308.

Hirokawa N, Tanaka Y, Okada Y. 2012. Cilia, KIF3 molecular motor and nodal flow. Curr Opin Cell Biol 24:31–39.

Houtmeyers R, Souopgui J, Tejpar S, Arkell R. 2013. The ZIC gene family encodes multi-functional proteins essential for patterning and morphogenesis. CMLS 70:3791–3811.

Lee JD, Anderson KV. 2008. Morphogenesis of the node and notochord: The cellular basis for the establishment and maintenance of left-right asymmetry in the mouse. Dev Dyn 237:3464–3476.

Lowe LA, Supp DM, Sampath K, Yokoyama T, Wright CV, Potter SS, Overbeek P, Kuehn MR. 1996. Conserved left-right asymmetry of nodal expression and alterations in murine situs inversus. Nature 381: 158–161.

Marques S, Borges AC, Silva AC, Freitas S, Cordenonsi M, Belo JA. 2004. The activity of the Nodal antagonist Cerl-2 in the mouse node is required for correct L/R body axis. Genes Dev 18:2342–2347.

Martin DM, Skidmore JM, Fox SE, Gage PJ, Camper SA. 2002. Pitx2 distinguishes subtypes of terminally differentiated neurons in the developing mouse neuroepithelium. Dev Biol 252:84–99.

McGrath J, Somlo S, Makova S, Tian X, Brueckner M. 2003. Two populations of node monocilia initiate left-right asymmetry in the mouse. Cell 114:61–73.

Meno C, Saijoh Y, Fujii H, Ikeda M, Yokoyama T, Yokoyama M, Toyoda Y, Hamada H. 1996. Left-right asymmetric expression of the TGF beta-family member lefty in mouse embryos. Nature 381:151–155.

Meno C, Shimono A, Saijoh Y, Yashiro K, Mochida K, Ohishi S, Noji S, Kondoh H, Hamada H. 1998. lefty-1 is required for left-right determination as a regulator of lefty-2 and nodal. Cell 94:287–297.

Moorman AF, Christoffels VM. 2003. Cardiac chamber formation: Development, genes, and evolution. Physiol Rev 83:1223–1267.

Nolan PM, Peters J, Strivens M, Rogers D, Hagan J, Spurr N, Gray IC, Vizor L, Brooker D, Whitehill E, Washbourne R, Hough T, Greenaway S, Hewitt M, Liu X, McCormack S, Pickford K, Selley R, Wells C, Tymowska-Lalanne Z, Roby P, Glenister P, Thornton C, Thaung C, Stevenson JA, Arkell R, Mburu P, Hardisty R, Kiernan A, Erven A, Steel KP, Voegeling S, Guenet JL, Nickols C, Sadri R, Nasse M, Isaacs A, Davies K, Browne M, Fisher EM, Martin J, Rastan S, Brown SD, Hunter J. 2000. A systematic, genome-wide, phenotype-driven mutagenesis programme for gene function studies in the mouse. Nat Genet 25:440–443.

Nonaka S, Shiratori H, Saijoh Y, Hamada H. 2002. Determination of left-right patterning of the mouse embryo by artificial nodal flow. Nature 418:96–99.

Nonaka S, Tanaka Y, Okada Y, Takeda S, Harada A, Kanai Y, Kido M, Hirokawa N. 1998. Randomization of left-right asymmetry due to loss of nodal cilia generating leftward flow of extraembryonic fluid in mice lacking KIF3B motor protein. Cell 95:829–837.

Norris DP. 2012. Cilia, calcium and the basis of left-right asymmetry. BMC Biol 10:102.

Pearce JJ, Penny G, Rossant J. 1999. A mouse cerberus/Dan-related gene family. Dev Biol 209:98–110.

Pennekamp P, Karcher C, Fischer A, Schweickert A, Skryabin B, Horst J, Blum M, Dworniczak B. 2002. The ion channel polycystin-2 is required for left-right axis determination in mice. Curr Biol 12:938–943.

Purandare SM, Ware SM, Kwan KM, Gebbia M, Bassi MT, Deng JM, Vogel H, Behringer RR, Belmont JW, Casey B. 2002. A complex syndrome of left-right axis, central nervous system and axial skeleton defects in Zic3 mutant mice. Development 129:2293–2302.

Roessler E, Lacbawan F, Dubourg C, Paulussen A, Herbergs J, Hehr U, Bendavid C, Zhou N, Ouspenskaia M, Bale S, Odent S, David V, Muenke M. 2009. The full spectrum of holoprosencephaly-associated mutations within the ZIC2 gene in humans predicts loss-of-function as the predominant disease mechanism. Hum Mutat 30:E541–554.

Ryan AK, Blumberg B, Rodriguez-Esteban C, Yonei-Tamura S, Tamura K, Tsukui T, de la Pena J, Sabbagh W, Greenwald J, Choe S, Norris DP, Robertson EJ, Evans RM, Rosenfeld MG, Izpisua Belmonte JC. 1998. Pitx2 determines left-right asymmetry of internal organs in vertebrates. Nature 394:545–551.

Shinohara K, Kawasumi A, Takamatsu A, Yoshiba S, Botilde Y, Motoyama N, Reith W, Durand B, Shiratori H, Hamada H. 2012. Two rotating cilia in the node cavity are sufficient to break left-right symmetry in the mouse embryo. Nat Commun 3:622.

Shiratori H, Hamada H. 2006. The left-right axis in the mouse: From origin to morphology. Development 133:2095–2104.

Shiratori H, Yashiro K, Shen MM, Hamada H. 2006. Conserved regulation and role of Pitx2 in situs-specific morphogenesis of visceral organs. Development 133:3015–3025.

Solomon BD, Lacbawan F, Mercier S, Clegg NJ, Delgado MR, Rosenbaum K, Dubourg C, David V, Olney AH, Wehner LE, Hehr U, Bale S, Paulussen A, Smeets HJ, Hardisty E, Tylki-Szymanska A, Pronicka E, Clemens M, McPherson E, Hennekam RC, Hahn J, Stashinko E, Levey E, Wieczorek D, Roeder E, Schell-Apacik CC, Booth CW, Thomas RL, Kenwrick S, Cummings DA, Bous SM, Keaton A, Balog JZ, Hadley D, Zhou N, Long R, Velez JI, Pineda-Alvarez DE, Odent S, Roessler E, Muenke M. 2010. Mutations in ZIC2 in human holoprosencephaly: Description of a novel ZIC2 specific phenotype and comprehensive analysis of 157 individuals. J Med Genet 47:513–524.

Sulik K, Dehart DB, Inagaki T, Carson JL, Vrablic T, Gesteland K, Schoenwolf GC. 1994. Morphogenesis of the Murine Node and Notochordal Plate. Dev Dyn 201:260–278.

Sutherland MJ, Wang SY, Quinn ME, Haaning A, Ware SM. 2013. Zic3 is required in the migrating primitive streak for node morphogenesis and leftright patterning. Human Mol Gen 22:1913–1923.

Thomas J, Morle L, Soulavie F, Laurencon A, Sagnol S, Durand B. 2010. Transcriptional control of genes involved in ciliogenesis: A first step in making cilia. Biol Cell 102:499–513.

Thomsen N, Ali RG, Ahmed JN, Arkell RM. 2012. High resolution melt analysis (HRMA); a viable alternative to agarose gel electrophoresis for mouse genotyping. PloS One 7:e45252.

Viotti M, Niu L, Shi SH, Hadjantonakis AK. 2012. Role of the gut endoderm in relaying left-right patterning in mice. PLoS Biol 10:e1001276.

Ware SM, Harutyunyan KG, Belmont JW. 2006. Heart defects in X-linked heterotaxy: Evidence for a genetic interaction of Zic3 with the nodal signaling pathway. Dev Dyn 235:1631–1637.

Warr N, Powles-Glover N, Chappell A, Robson J, Norris D, Arkell RM. 2008. Zic2-associated holoprosencephaly is caused by a transient defect in the organizer region during gastrulation. Hum Mol Genet 17: 2986–2996.

Yamamoto M, Mine N, Mochida K, Sakai Y, Saijoh Y, Meno C, Hamada H. 2003. Nodal signaling induces the midline barrier by activating Nodal expression in the lateral plate. Development 130:1795–1804.

Yoshiba S, Shiratori H, Kuo IY, Kawasumi A, Shinohara K, Nonaka S, Asai Y, Sasaki G, Belo JA, Sasaki H, Nakai J, Dworniczak B, Ehrlich BE, Pennekamp P, Hamada H. 2012. Cilia at the Node of Mouse Embryos Sense Fluid Flow for Left-Right Determination via Pkd2. Science 338:226–231.

Zhang M, Bolfing MF, Knowles HJ, Karnes H, Hackett BP. 2004. Foxj1 regulates asymmetric gene expression during left-right axis patterning in mice. Biochem Biophys Res Commun 324:1413–1420.